

## Supporting Information

To

### **Engineered Holliday Junctions as Single-Molecule Reporters for Protein-DNA Interactions with Application to a MerR-family Regulator**

Susanta K. Sarkar,<sup>a</sup> Nesha May Andoy,<sup>a</sup> Jaime J. Benítez,<sup>a</sup> Peng R. Chen,<sup>b</sup>  
Jason S. Kong,<sup>a</sup> Chuan He,<sup>b</sup> Peng Chen<sup>a,\*</sup>

<sup>a</sup> Department of Chemistry and Chemical Biology, Baker Laboratory, Cornell University,  
Ithaca, NY 14853. <sup>b</sup> Department of Chemistry, University of Chicago, 929 E 57th Street,  
Chicago, IL 60637

\* Corresponding Author:

Peng Chen

Department of Chemistry and Chemical Biology, Baker Laboratory

Cornell University, Ithaca, NY 14850

Phone: 607-254-8533, Fax: 607-255-4137

E-mail: pc252@cornell.edu

### Control experiments for smFRET measurements in the presence of Pb<sup>2+</sup>.

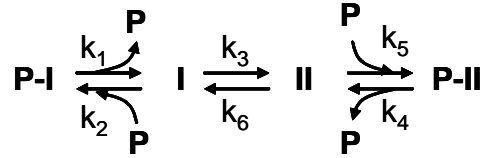
Trolox is a reducing agent and could potentially reduce Pb<sup>2+</sup> in our smFRET experiments. Although no structural data are available for PbrR691, Pb<sup>2+</sup> is possibly bound by cysteine ligands inside the protein. Consistently, upon adding Pb<sup>2+</sup> (i.e., Pb(NO<sub>3</sub>)<sub>2</sub>) to PbrR691, a charge transfer band appears at ~340 nm (Figure S12A), a typical spectral location for thiolate to Pb<sup>2+</sup> charge transfer transitions.<sup>1</sup> This absorption saturates at [Pb<sup>2+</sup>]:[PbrR691] = 1:1 (Figure S12B), consistent with the Pb<sup>2+</sup> binding stoichiometry of PbrR691.<sup>2</sup> In the presence of 1 mM Trolox, same concentration as used in our smFRET experiments, this charge transfer persists (Figure S12A), indicating the Pb<sup>2+</sup> is not reduced by Trolox and stays bound to the protein. We also investigated HJ1 structural dynamics in the presence of Pb<sup>2+</sup> in the solution. No significant difference was observed in its interconversion kinetics (Figure S13).

**Derivation of expression for fitting the titration curve in Figure 4.** The E<sub>FRET</sub> peak area ratio  $r$  in Figure 4 represents the ensemble equilibrium distribution of conf-I and conf-II of HJ1. In the presence of PbrR691, the area ratio should be:

$$r = \frac{[\text{I}] + [\text{P - I}]}{[\text{II}] + [\text{P - II}]} = \frac{[\text{I}]}{[\text{II}]} \left( \frac{1 + \frac{[\text{P - I}]}{[\text{I}]}}{1 + \frac{[\text{P - II}]}{[\text{II}]}} \right) = C \left( 1 + \frac{[\text{P}]}{K_{D-I}} \right) / \left( 1 + \frac{[\text{P}]}{K_{D-II}} \right) \quad [1]$$

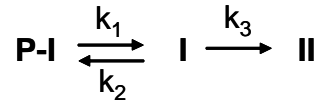
where I represents conf-I of HJ1, II represents conf-II, and P represents PbrR691. P-I and P-II are the PbrR691-conf-I and PbrR691-conf-II complexes respectively, C is the area ratio of conf-I/conf-II in the E<sub>FRET</sub> trajectory histogram of free HJ1.

**Possibility of HJ1 structural interconversion involving complete dissociation of PbrR691.** The structural interconversion between PbrR691 bound conf-I and conf-II could involve complete dissociation of PbrR691 from HJ1 and then re-association of PbrR691, as shown in the following scheme:



where I represents conf-I of HJ1, II represents conf-II, and P represents PbrR691. P-I and P-II are the PbrR691-conf-I and PbrR691-conf-II complexes respectively. The rate constants are also indicated for all steps. Rate constants  $k_3$  and  $k_6$  can be obtained from the waiting time distributions of free HJ1 molecules (Figure 3B, C).

To compute the distribution,  $f_{\text{conf-I}}(t)$ , of the waiting time  $t_{\text{conf-I}}$ , we need to consider the following half reaction,

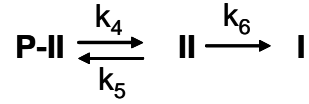


which describes the reaction steps for the structural transition from P-I to II (free protein, P, is omitted for simplicity in the scheme). It has been shown for the above kinetic scheme,<sup>3-5</sup>  $f_{\text{conf-I}}(t)$  has the following form,

$$f_{\text{conf-I}}(t) = \frac{k_1 k_3}{2A} [\exp(A + B)t - \exp(B - A)t] \quad [2]$$

where  $A = \sqrt{(k_1 + k_2[P] + k_3)^2 / 4 - k_1 k_3}$ ,  $B = -(k_1 + k_2[P] + k_3) / 2$ , and  $[P]$  is the PbrR691 concentration.

Similarly, to compute the distribution,  $f_{\text{conf-II}}(t)$ , of the waiting time  $t_{\text{conf-II}}$ , we need to consider the following half reaction,



and then  $f_{\text{conf-II}}(t)$  is,

$$f_{\text{conf-II}}(t) = \frac{k_4 k_6}{2A} [\exp(A + B)t - \exp(B - A)t] \quad [3]$$

where  $A = \sqrt{(k_4 + k_5[\text{P}] + k_6)^2 / 4 - k_4 k_6}$ ,  $B = -(k_4 + k_5[\text{P}] + k_6) / 2$ .

The distributions of the waiting time  $t_{\text{conf-I}}$  and  $t_{\text{conf-II}}$  could be fitted by equations [2] and [3] (Figure S1). However, the fitting results are clearly unreliable, indicated by the huge errors of fitted values of  $k_1$ ,  $k_2$ ,  $k_4$ , and  $k_5$ . In fact, using the fitting algorithms in MatLab, all fittings for different protein concentrations could not be converged. Attempts of fixing the  $k_1/k_2$  and  $k_3/k_4$  ratios to  $K_{\text{D-I}}$  and  $K_{\text{D-II}}$  determined from  $E_{\text{FRET}}$  histogram titration (Figure 4B, inset) did not get reliable fits either. Therefore, our data do not warrant a reliable analysis assuming this pathway for structural interconversion between the two PbrR691 bound conformers of HJ1, although we cannot rule out this possibility. To provide reliable kinetics for the structural transitions, we analyzed the waiting time distributions of HJ1 in the presence of PbrR691 by decomposing them into two exponential components. One of them accounts for the population of free HJ1 and the other with PbrR691 bound, as presented in the text (Figure 3).

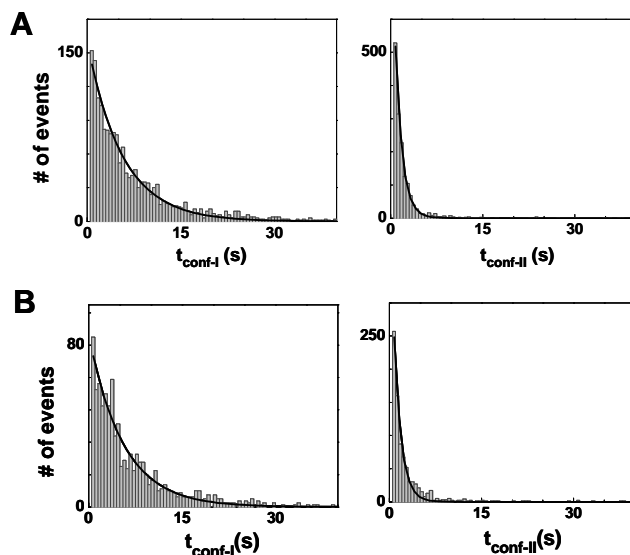


**Figure S1.** Waiting time distributions of HJ1 in the presence of (A) 2.4  $\mu\text{M}$  and (B) 0.3  $\mu\text{M}$  apo-PbrR691. Bin size: 0.5 s. Solid lines are fits using equations [2] and [3].

Fit parameters: (A) Left:  $k_1 = 11 \pm 414 \text{ s}^{-1}$   
 $k_2 = 0.5 \pm 18 \text{ s}^{-1}$   
 $k_3 = 0.21 \text{ s}^{-1}$  (fixed at the value for free HJ1)  
 Right:  $k_4 = 14 \pm 116 \text{ s}^{-1}$   
 $k_5 = 0 \pm 15 \text{ s}^{-1}$   
 $k_6 = 0.58 \text{ s}^{-1}$  (fixed at the value for free HJ1)

(B) Left:  $k_1 = 1300 \pm 2\text{e}6 \text{ s}^{-1}$   
 $k_2 = 312 \pm 4\text{e}5 \text{ s}^{-1}$   
 $k_3 = 0.21 \text{ s}^{-1}$  (fixed at the value for free HJ1)  
 Right:  $k_4 = 1750 \pm 25\text{e}6 \text{ s}^{-1}$   
 $k_5 = 0 \pm 21\text{e}6 \text{ s}^{-1}$   
 $k_6 = 0.58 \text{ s}^{-1}$  (fixed at the value for free HJ1)

## References

- (1) Matzapetakis, M.; Ghosh, D.; Weng, T.-C.; Penner-Hahn, J. E.; Pecoraro, V. L. *J. Biol. Inorg. Chem.* **2006**, *11*, 876.
- (2) Chen, P.; Greenberg, B.; Taghavi, S.; Romano, C.; van der Lelie, D.; He, C. *Angew. Chem., Int. Ed.* **2005**, *44*, 2715.
- (3) Lu, H. P.; Xun, L. Y.; Xie, X. S. *Science* **1998**, *282*, 1877.
- (4) Xie, X. S. *Single Mol.* **2001**, *2*, 229.
- (5) Kou, S. C.; Cherayil, B. J.; Min, W.; English, B. P.; Xie, X. S. *J. Phys. Chem. B* **2005**, *109*, 19068.

## More Supporting Figures



**Figure S2.** Structure model of HJ1 with the dyad symmetric sequence highlighted in red as in conf-II.

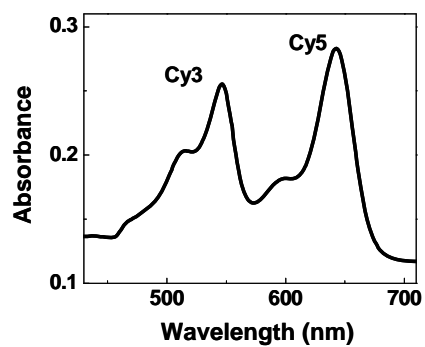


**Figure S3.** Absorption spectrum of HJ1. The intensities of Cy3 and Cy5 absorption bands indicate their 1:1 molar ratio, further confirming the assembly of HJ1.

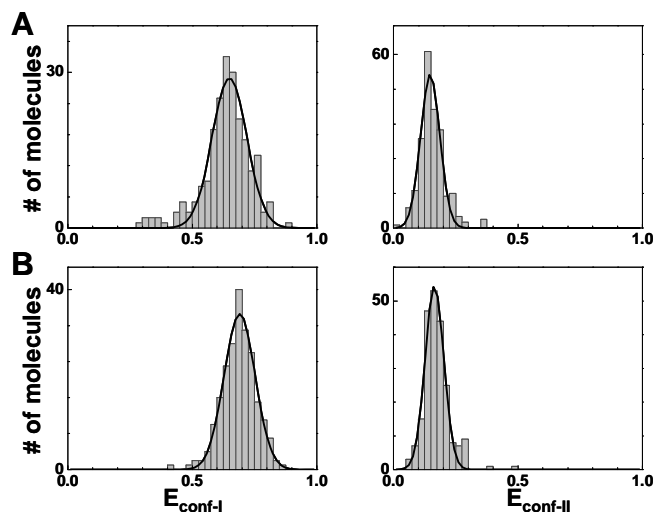


**Figure S4.** Histograms of  $E_{\text{conf-I}}$  and  $E_{\text{conf-II}}$  of HJ1 in the absence (A) and presence of 2.4  $\mu\text{M}$  apo-PbrR691 (B). The  $E$  values were obtained by fitting the individual histograms of the  $E_{\text{FRET}}$  trajectories with two Gaussian functions. Each histogram was compiled from 220 HJ1 molecules. Bin size: 0.025.

Fit parameters: (A) left,  $E_{\text{conf-I}} = 0.649 \pm 0.003$ ,  $\text{FWHM} = 0.165 \pm 0.007$ ;  
 right,  $E_{\text{conf-II}} = 0.148 \pm 0.002$ ,  $\text{FWHM} = 0.092 \pm 0.005$ ;  
 (B) left,  $E_{\text{conf-I}} = 0.690 \pm 0.002$ ,  $\text{FWHM} = 0.146 \pm 0.005$ ;  
 right,  $E_{\text{conf-II}} = 0.165 \pm 0.001$ ,  $\text{FWHM} = 0.090 \pm 0.002$ .

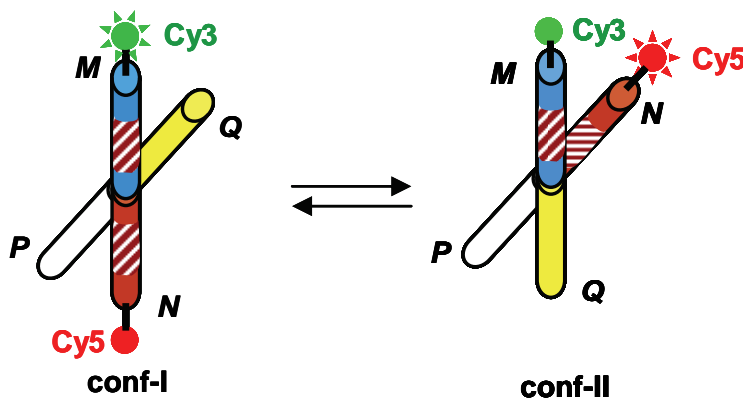


**Figure S5.** Structural dynamics of HJ1a with alternative labeling.

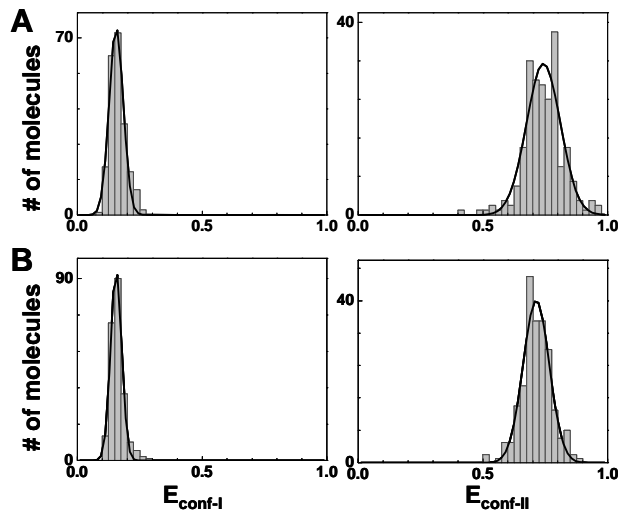


**Figure S6.** Histograms of  $E_{\text{conf-I}}$  and  $E_{\text{conf-II}}$  of the alternatively labeled HJ1a in the absence (A) and presence of 2.4  $\mu\text{M}$  apo-PbrR691 (B). The E values were obtained by fitting the individual histograms of the  $E_{\text{FRET}}$  trajectories with two Gaussian functions. Each histogram was compiled from 220 HJ1a molecules. Bin size: 0.025.

Fit parameters: (A) left,  $E_{\text{conf-I}} = 0.156 \pm 0.001$ ,  $\text{FWHM} = 0.066 \pm 0.002$ ;  
 right,  $E_{\text{conf-II}} = 0.742 \pm 0.005$ ,  $\text{FWHM} = 0.160 \pm 0.012$ ;  
 (B) left,  $E_{\text{conf-I}} = 0.156 \pm 0.000$ ,  $\text{FWHM} = 0.052 \pm 0.002$ ;  
 right,  $E_{\text{conf-II}} = 0.713 \pm 0.002$ ,  $\text{FWHM} = 0.123 \pm 0.005$ .

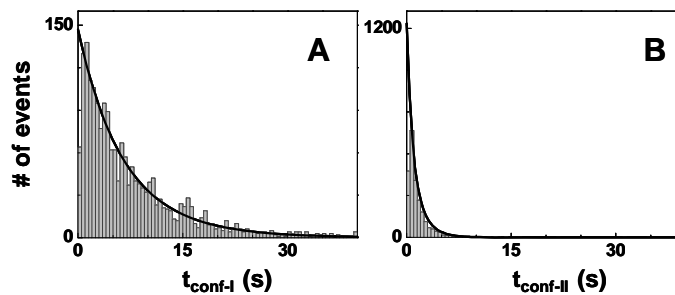


**Figure S7.** Waiting time distributions of HJ1 in the presence of 2.4  $\mu\text{M}$  PbrR691 and 4.0  $\mu\text{M}$   $\text{Pb}^{2+}$ . Data were from trajectories of 229 molecules. Bin size: 0.5 s. Solid lines in are fits with  $y = A\exp(-kt) + A'\exp(-k't)$ .

Fit parameters: (A)  $A = 16 \pm 1$ ,  $k = 0.20 \pm 0.01 \text{ s}^{-1}$ ,  $A' = 133 \pm 3$ ,  $k' = 0.14 \pm 0.01 \text{ s}^{-1}$ .  
 (B)  $A = 295 \pm 7$ ,  $k = 0.58 \pm 0.02 \text{ s}^{-1}$ ,  $A' = 1231 \pm 29$ ,  $k' = 1.42 \pm 0.04 \text{ s}^{-1}$ .

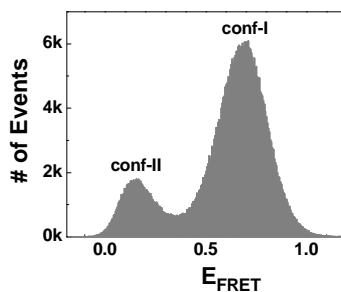


**Figure S8.**  $E_{\text{FRET}}$  trajectory histograms of HJ1 in the presence of 2.4  $\mu\text{M}$  PbrR691 and 4.0  $\mu\text{M}$   $\text{Pb}^{2+}$ . Data compiled from trajectories of 229 molecules. Bin size: 0.005.

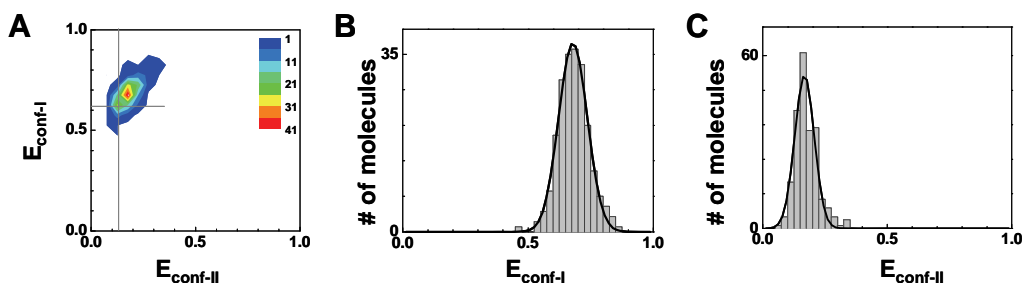


**Figure S9.** 2-dimensional (A) and 1-dimensional (B, C) histograms of  $E_{\text{conf-I}}$  and  $E_{\text{conf-II}}$  of HJ1 in the presence of 2.4  $\mu\text{M}$  PbrR691 and 4.0  $\mu\text{M}$   $\text{Pb}^{2+}$ . The E values were obtained by fitting the individual histograms of the  $E_{\text{FRET}}$  trajectories with two Gaussian functions. Data compiled from 217 molecules. Bin size: 0.05 (A) and 0.025 (B, C).

Fit parameters: (B)  $E_{\text{conf-I}} = 0.680 \pm 0.001$ , FWHM =  $0.134 \pm 0.002$ .

(C)  $E_{\text{conf-II}} = 0.167 \pm 0.002$ , FWHM =  $0.092 \pm 0.005$ .

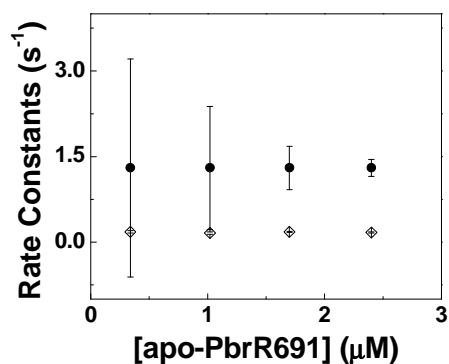


**Figure S10.** Apo-PbrR691 concentration dependence of the rate constants for structural transitions between protein bound HJ1 conformers. Diamonds,  $k'_{\text{I} \rightarrow \text{II}}$ ; black dots,  $k'_{\text{II} \rightarrow \text{I}}$ .

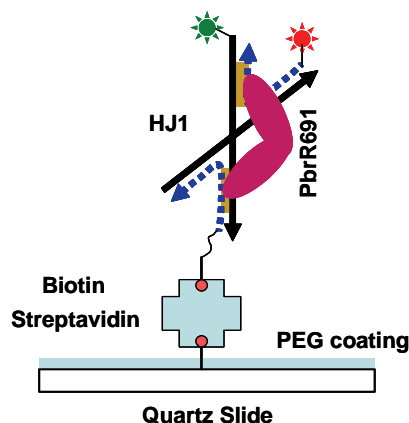


**Figure S11.** Scheme of immobilization of HJs in single-molecule fluorescence measurements.

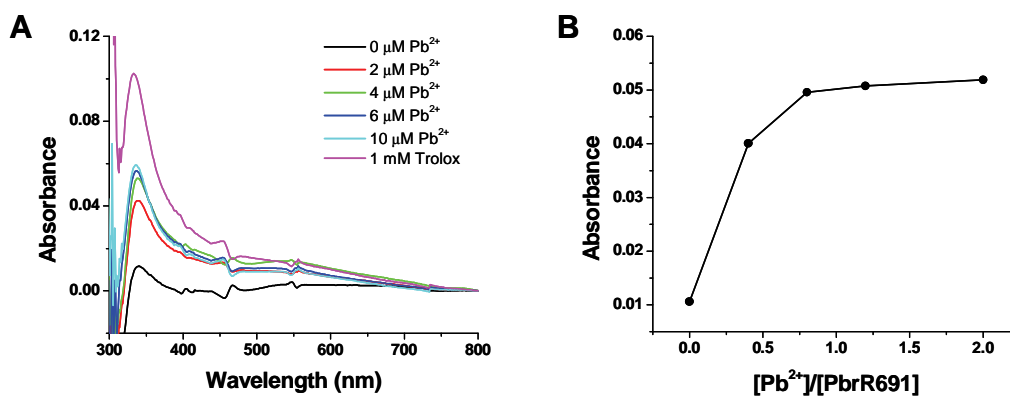


**Figure S12.** Absorption spectra of PbrR691 with increasing  $[Pb^{2+}]$ .  $[PbrR691] = 5 \mu M$ . The large absorbance increase upon addition of Trolox in (A) is due to an absorption band of Trolox at  $<300$  nm.

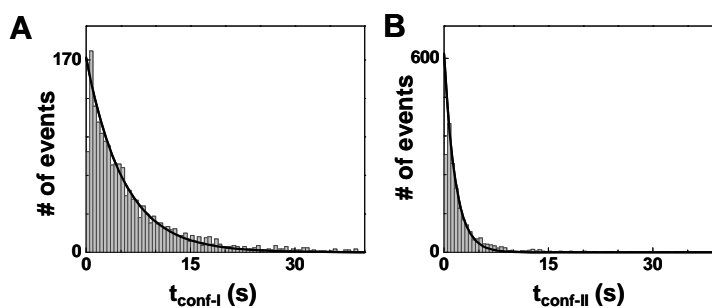


**Figure S13.** Waiting time distributions of HJ1 in the presence of  $4.0 \mu M Pb^{2+}$ . Data were from trajectories of 220 molecules. Bin size: 0.5 s. Solid lines in are fits with  $y = Aexp(-kt)$ . Fit parameters: (A)  $k = 0.19 \pm 0.01 s^{-1}$ , (B)  $k = 0.62 \pm 0.01 s^{-1}$ .

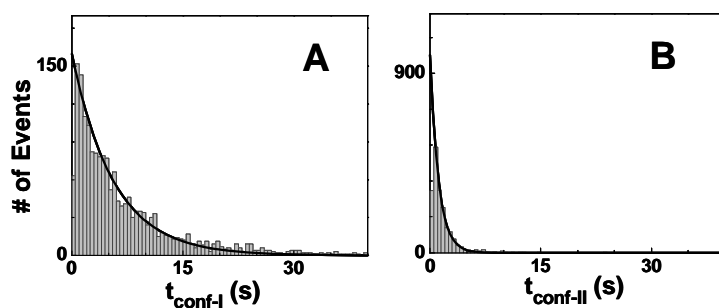


**Figure S14.** Fitting of Figure 3E and F with the single-exponential function  $y = A\exp(-kt)$ . Fit parameters: (A)  $A = 160 \pm 3$ ,  $k = 0.17 \pm 0.01 \text{ s}^{-1}$ , (B)  $A = 992 \pm 13$ ,  $k = 0.87 \pm 0.01 \text{ s}^{-1}$ .

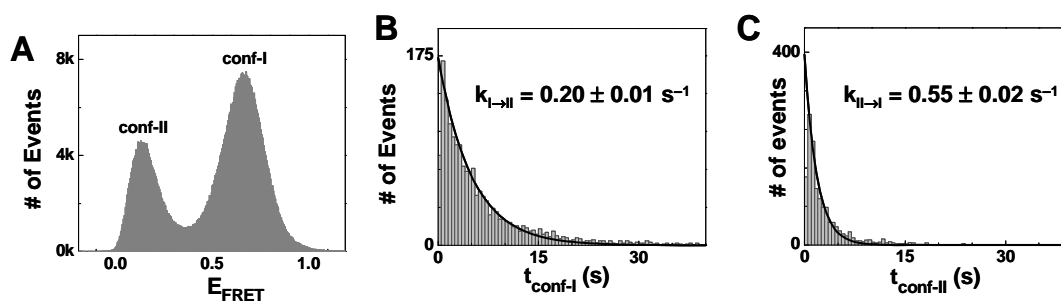


**Figure S15.** (A)  $E_{\text{FRET}}$  trajectory histograms of HJ1 in the presence of  $5.0 \mu\text{M}$  apo-CueR. No noticeable perturbation of the HJ1 structural equilibrium by CueR was observed, as compared to Figure 4A. Data compiled from trajectories of 285 molecules. Bin size: 0.005. (B) and (C) Waiting time distributions of HJ1 in the presence of  $5.0 \mu\text{M}$  apo-CueR. Bin size, 0.5 s. The rate constants are from single-exponential fits. No significant changes of the transition rates were observed as compared to those of free HJ1 in Figures 3B and C.

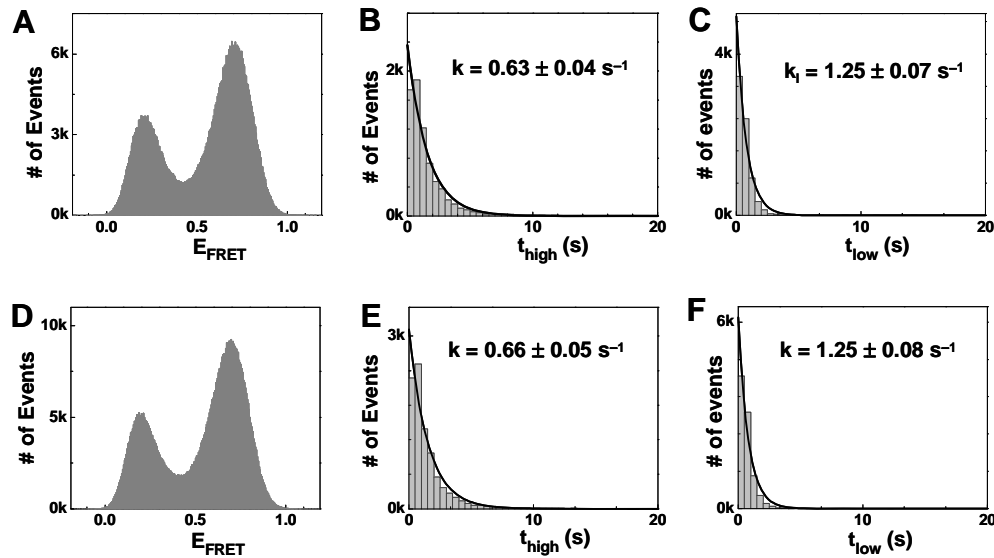


**Figure S16.**  $E_{\text{FRET}}$  trajectory histograms of a Holliday junction (J7) that contains no protein-targeting sequence in the absence (A) and in the presence (D) 2.4  $\mu\text{M}$  apo-PbrR691. No noticeable perturbation of the J7 of the structural equilibrium by PbrR691 was observed. Data compiled from trajectories of 253 and 343 molecules for (A) and (D) respectively. Bin size: 0.005. (B, C) Waiting time distributions of free J7. Bin size, 0.5 s. (E, F) Waiting time distributions of J7 in the presence of 2.4  $\mu\text{M}$  apo-PbrR691. No significant changes of the transition rates were observed as compared to those of free J7. Bins size, 0.5 s.

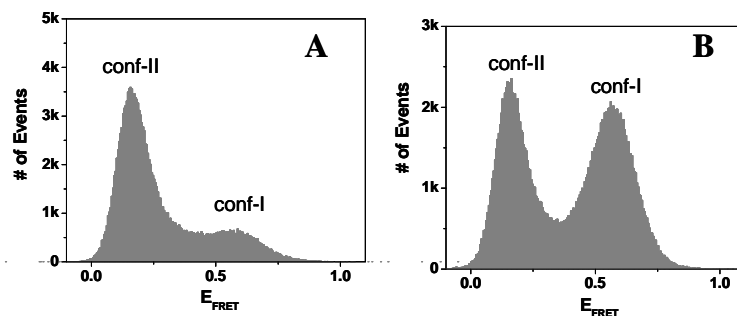


**Figure S17.**  $E_{\text{FRET}}$  trajectory histograms of an engineered Holliday junction that contains the dyad sequence recognized by the MerR-family regulator CueR in the absence (A) and presence (B) 1.0  $\mu\text{M}$  apo-CueR. Data compiled from trajectories of 120 molecules for each histogram. Bin size: 0.005. The relative intensity of the peak corresponding to conf-I increases dramatically upon CueR interaction, consistent with the observations for HJ1-PbrR691 interactions. This exemplifies the applicability and generalizability of our approach using engineered Holliday junctions to probe protein-DNA interactions. The experiments were done in Tris/ $\text{HNO}_3$  buffer, pH7.3, 80 mM  $\text{Na}^+$ , and 2 mM  $\text{Mg}^{2+}$ . The detailed study on CueR will be published separately.